JOURNAL OF CATALYSIS 78, 24–33 (1982)

The Role of Carbon and Oxygen in the Activation of an Iron Fischer–Tropsch Catalyst at Low Pressures

WIM L. VAN DIJK[1] AND HESSEL S. VAN DER BAAN

Laboratory for Chemical Technology, Eindhoven University of Technology, The Netherlands

Received September 22, 1981; revised March 5, 1982

The Fischer–Tropsch synthesis was studied at 520 K on reduced iron catalysts at a pressure of 24 Pa in a continuous-flow fixed-bed reactor and at 9 kPa in a batch reactor. A quadrupole analyzer detector was used for continuous monitoring of the products formed. In the experiments at 24 Pa a preference for the formation of aromatics was observed. From this it is concluded that carbon adsorption on sites next to an occupied site is favoured as compared to adsorption on a clean part of the surface. In experiments at 9 kPa very little activity is observed for a period of about 15 ks, after which the customary activation sets in. However, when the catalyst is pretreated with a small quantity of oxygen, hydrocarbons up to C_6 and C_7 compounds are produced immediately. Consequently, the activation is also associated with the presence of oxygen on the catalyst. The activation is ascribed to the formation of certain active hydrogenation ensembles which form faster on the preoxidized catalyst. From preoxidation experiments with $^{18}O_2$ it is concluded that the rate of dissociation of carbon monoxide on iron catalysts is a fast reaction compared to the overall Fischer–Tropsch reaction rate.

INTRODUCTION

When freshly reduced iron catalysts are exposed to synthesis gas the rate of hydrocarbon production increases in the course of an experiment from zero to a maximum and finally levels off at a value below that maximum. It has been found that during this activation a considerable uptake of carbon and oxygen occurs (*1*). This process is rather fast under atmospheric conditions. In order to study these depositions in more detail, we have followed the activation of an iron-based Fischer–Tropsch catalyst at low pressures, where all processes proceed at a much lower rate. For this a high-vacuum system was built, with the reactor directly coupled to a quadrupole mass spectrometer. With this system quantitative data could be obtained at low reactant pressures.

Tillmetz (*2*) has already given a partly quantitative description of the reaction at very low pressures (10^{-2}–10^{-5} Pa) on fully carbided iron catalysts. On rhodium polycrystalline foils Sexton and Somorjai (*3*) were not able to produce meaningful data at such low pressures, because the amounts of higher hydrocarbons produced were too small for reliable detection by a quadrupole analyzer. At these extremely low pressures also our experiments with iron catalysts were unsuccessful. Therefore our experiments were carried out at pressures between 10 and 10^4 Pa.

We have used for this study an iron manganese oxide catalyst as this study is part of an investigation into the effect of manganese oxide on the olefin selectivity of iron catalysts (*1*, *9*). In the latter publication it is shown that the iron/manganese oxide catalyst used in the present study behaves very much like a pure precipitated iron catalyst.

EXPERIMENTAL

High-Vacuum Apparatus

A general scheme of the apparatus is shown in Fig. 1. The system consists of a feed section, a reaction section, and a quadrupole section.

---

[1] Present address: ESSO Nederland BV, Rotterdam, The Netherlands.

0021-9517/82/110024-10$02.00/0
Copyright © 1982 by Academic Press, Inc.
All rights of reproduction in any form reserved.

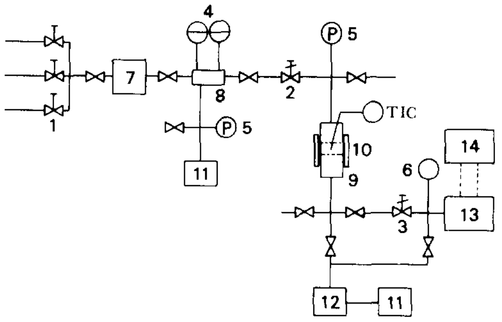

FIG. 1. Scheme of the high-vacuum apparatus. 1 mass flow controllers, 2 and 3 variable leak valves, 4 differential pressure gauges, 5 thermal conductivity pressure gauges, 6 ionization pressure gauge, 7 mixing vessel, 8 feed vessel, 9 reactor, 10 oven, 11 rotary vane pumps, 12 turbomolecular pump, 13 quadrupole analyzer, and 14 microprocessor.

The complete apparatus was made of stainless-steel (AISI 316/321) Leybold–Heraeus equipment parts and the connections were sealed with copper gaskets. All the equipment has been baked out at 575 K. During Fischer–Tropsch synthesis the whole system is kept at 420 K, except the reactor which is kept at 525 K.

The reaction mixture is prepared in the feed section. The reactor operates at 24 Pa as a fixed-bed flow reactor and at 9 kPa as a batch reactor.

Gas mixtures of H_2, CO, and Ne are prepared by separate regulation of each gas stream with mass flow controllers 1 (Brooks 5841-1) and stored in a feed volume of 63 cm^3. The absolute pressure in this feed volume is determined by a membrane differential pressure gauge PD 1.0 (Hottinger Baldwin; 10^2–10^5 Pa). When the reactor is used as a continuous-flow fixed-bed reactor, the gas feed rate into the reactor is calculated from the rate of pressure decrease in the feed volume. This pressure decrease is followed by a PD 0.01 differential pressure gauge (measuring range 1 to 10^3 Pa).

The gases hydrogen (Matheson, ultrahigh purity >99.999%), carbon monoxide (Matheson, purity >99.997%), and neon (Hoekloos, purity >99.9%) were used as supplied.

For the continuous-flow experiments at 24 Pa the gas mixture is admitted to the reactor by variable (Leybold–Heraeus) leak valve 2, which maintains a constant feed rate into the reactor, as long as the pressure in the feed section does not change too much. The pressure in the reactor is controlled by a second variable leak valve, 3, which connects the reactor to the quadrupole section. The ratio of the concentrations of the various components to that of neon, determined with the quadrupole, was used to calculate the mole fractions at the outlet of the reactor. The reaction rate was calculated by multiplying these mole fractions by the gas feed rate.

At the higher pressure of 9 kPa the pumping system operating at 10^{-4} Pa is unable to maintain an acceptable feed rate through the reactor. Consequently the reactor is operated as a batch reactor at this pressure. The total reactor volume in this case is 1.8 dm^3. From the reactor a small sample flow is admitted via variable leak valve 3 to the quadrupole section, kept at a pressure between 10^{-3} and 10^{-4} Pa. From the fast stepwise increase of some concentrations at the beginning of an experiment we conclude that concentration gradients in the reactor can be neglected in this study. The reactor is made of quartz glass and was filled with 1 g of unreduced catalyst. A bypass line around valve 3 is used for fast evacuation of the reactor after reduction of the catalyst or after a Fischer–Tropsch experiment. The pressure in the reactor is measured with thermal conductivity vacuum gauge 5 (Leybold–Heraeus, Thermotron 11/12, range 1 to 10^4 Pa).

A simple quadrupole mass spectrometer (Leybold–Heraeus, Quadruvac Q 200, mass range 0–100 amu) was chosen as analyzer. A Puzzle PSDS 20 microcomputer was adapted to control the scan over a selected mass range of the quadrupole and to choose for each mass signal the appropriate amplifier range, providing a total dynamic range of 10^5 over the complete mass spectrum. The intensity at each mass was measured 16 times and the mean value printed in the output.

At high sensitivities the leading edge of a strong peak can extend into the region of a preceding small peak. A mathematical procedure was then applied to obtain an estimate of the small peak. Complete details will be published elsewhere (*4*). The quadrupole mass spectrometer is calibrated by admitting mixtures of known compositions into the quadrupole section. The intensities (relative to neon) for the main peak of each component are presented in Table 1.

A computer program, based on a modification of a stepwise linear regression program, that gives both qualitative and quantitative data for the composition of a sample has been developed by Henriquez (*5*, *6*). This program uses the spectra of a great number of possible components stored in a library. Since no oxygen-containing hydrocarbons were chosen from the library by the linear regression procedure, these compounds were not present in statistically significant quantities in our experiments.

Catalyst Preparation and Pretreatments

An iron manganese oxide catalyst with an iron-to-manganese atomic ratio of 4 : 1 was used in most of the experiments. The iron manganese oxide catalysts were prepared by slowly adding ammonium hydroxide (12% by wt ammonia, Merck P.A., 0.05 cm^3/s) to a solution (3 dm^3) of 0.25 kmol/m^3 iron (III) nitrate ($Fe(NO_3)_3 \cdot 9H_2O$, Merck P.A.) and 0.06 kmol/m^3 manganese (II) nitrate ($Mn(NO_3)_2 \cdot 4H_2O$, Riedel P.A.), which was heated to 365 K. The ammonia addition was stopped when a pH of 8 was reached. The precipitate was filtered off and washed with 200 cm^3 distilled water. It was then dried at 390 K for 86 ks and calcined at 675 K for 4 ks. In all the experiments 1 g of this calcined product with a sieve fraction of 0.2–0.6 mm was used.

Standard reduction of the catalyst was carried out at 625 K in flowing hydrogen (1.7 cm^3/s) for 70 ks. After this, an estimated 90% of the iron is present in the form of zerovalent iron. The remaining iron, Fe^{2+} and Fe^{3+}, is presumably associated with the manganese oxide in the catalyst (*9*), which is present as MnO. Thereafter the reactor was quickly evacuated and cooled to the reaction temperature of 525 K. Evacuation was continued for about 15 ks until a pressure of about 10^{-4} Pa was obtained in the reactor. The reduced catalyst contained 56% by wt of iron.

TABLE 1

Sensitivities of a Quadrupole Equipped with a Multiplier for the Main Peak of Various Compounds with Respect to Neon

Component	Sensitivity	Component	Sensitivity
Xylene	3.5[a]	Propene	2.9
Toluene	3.5[a]	Ethane	3.4
Benzene	3.5[a]	Ethene	3.4
Heptane	3.4[a]	Methane	3.6
Heptene-1	3.4[a]	Argon	3.7
Hexane	3.3[a]	Water	3.3[a]
Hexene-1	3.3[a]	Neon	1.0
Pentane	3.3[a]	Carbon dioxide	2.6
Pentene-1	3.3[a]	Carbon monoxide	4.2
Butane	3.2	Nitrogen	3.3
Butene-1	3.2	Hydrogen	5.0
Propane	2.9		

[a] Estimated values.

RESULTS

CO Hydrogenation over a Reduced Catalyst at 24 Pa

The Fischer–Tropsch reaction was investigated at 525 K and 24 Pa with a mixture of H_2, CO, and Ne with a volumetric ratio of 40 : 10 : 50 at a feed rate of 4.9 nmol/s. During the first period of about 30 ks the carbon monoxide was mainly converted into benzene and toluene, while the rate of formation of methane was much lower (see Fig. 2). Besides aromatic compounds also the olefins propene and butene and possibly ethene were formed. Formation of ethene could not be determined accurately, because the main peak coincides with that of carbon monoxide. The production of ben-

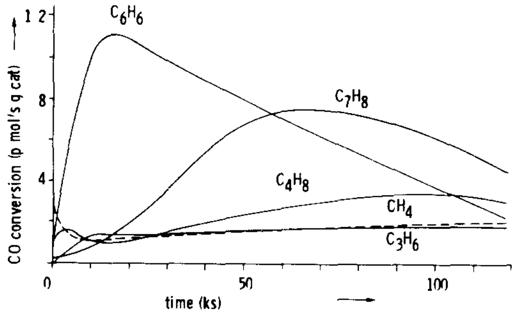

FIG. 2. Conversion rate of CO into various hydrocarbons during Fischer–Tropsch synthesis in the continuous-flow fixed-bed reactor. $T = 523$ K; $P_{H_2} = 9.6$ Pa; $P_{CO} = 2.4$ Pa.

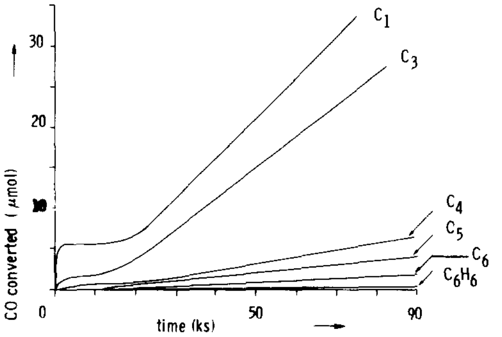

FIG. 4. Formation of various hydrocarbons during Fischer–Tropsch synthesis in a batch reactor. $T = 523$ K; $P_{H_2} = 5.5$ kPa; $P_{CO} = 1.4$ kPa; 1 g catalyst.

zene and toluene was much higher than that derived from a Schulz–Flory relation based on the C_1, C_3, and C_4 hydrocarbon formation rates.

Since all products and carbon monoxide were analyzed during the course of the synthesis, a mass balance for carbon and for oxygen could be obtained. The results of this calculation are shown in Fig. 3, indicating that the catalyst absorbed only small quantities of carbon and oxygen during the experiment.

CO Hydrogenation over a Reduced Catalyst at 9.2 kPa

The Fischer–Tropsch reaction was also investigated at 525 K and a pressure of 9.2 kPa with the reactor operating as a batch reactor. A 60 : 15 : 25 gas composition of H_2, CO, and Ne was used in this experiment.

Methane and to a much smaller extent hydrocarbons up to C_4 were formed immediately after the introduction of the synthesis mixture (see Fig. 4), possibly again with the hydrogen left on the catalyst after reduction. During the subsequent period of about 15 ks no further product was formed, although much carbon and oxygen were deposited during this period on the catalyst as followed from the mass balances (see Fig. 5). This deposition continued until about 0.8 mmol C/g Fe and 0.5 mmol O/g Fe were deposited on the catalyst. The concentrations of carbon monoxide, carbon dioxide, and water in the reactor are given in Fig. 6.

CO Hydrogenation over Preoxidized Catalysts at 9.2 kPa

When the Fischer–Tropsch synthesis was performed under atmospheric pressure conditions (*1*) or at lower pressures (see the preceding section), we observed during the activation of the catalyst not only the deposition of carbon but also a considerable uptake of oxygen. To investigate the influence

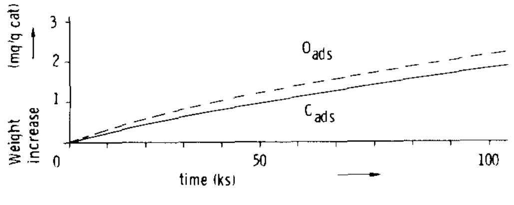

FIG. 3. Uptake of carbon and oxygen during Fischer–Tropsch synthesis in the continuous-flow fixed-bed reactor. $T = 523$ K; $P_{H_2} = 9.6$ Pa; $P_{CO} = 2.4$ Pa.

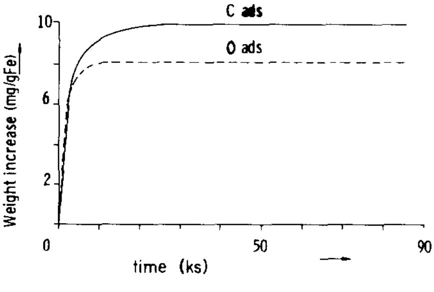

FIG. 5. Uptake of carbon and oxygen during Fischer–Tropsch synthesis in the batch reactor. $T = 523$ K; $P_{H_2} =$ kPa; $P_{CO} = 1.4$ kPa.

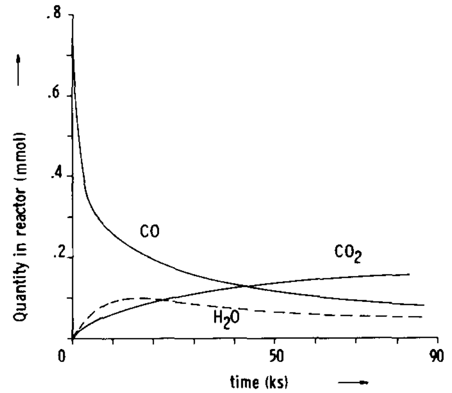

FIG. 6. Concentration of the products H_2O and CO_2 and the reactant carbon monoxide during Fischer–Tropsch synthesis in the batch reactor. Synthesis: $T = 523$ K; $P_{H_2} = 5.5$ kPa; $P_{CO} = 1.4$ kPa; 1 g catalyst.

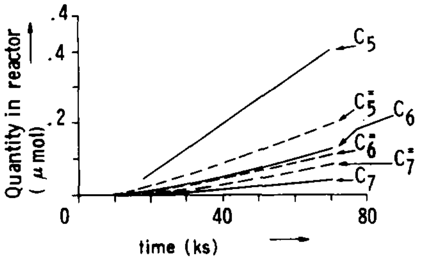

FIG. 8. C_5–C_7 olefin (C_n^{2-}) and paraffin (C_n) concentrations during Fischer–Tropsch synthesis on a reduced catalyst in the batch reactor. Synthesis: $T = 523$ K; $P_{H_2} = 5.5$ kPa; $P_{CO} = 1.4$ kPa.

of oxygen on the Fischer–Tropsch reaction, experiments were performed on preoxidized iron catalysts. The oxidation was carried out at room temperature by expanding a diluted 1.8% O_2/Ne mixture from the feed volume into the closed reactor (1.8 dm^3). Two different gas mixtures, which contained 40 and 70 μmol of oxygen, $^{16}O_2$ and $^{18}O_2$ respectively, were contacted with the standard quantity of reduced iron manganese oxide catalyst for a period of 1.7 and 11 ks, respectively. At the end of the pretreatment the reactor was quickly evacuated and thereafter in 2 ks heated to the reaction temperature of 525 K. The reaction was carried out again at 9.2 kPa and 525 K in the batch reactor system with a 60 : 15 : 25 gas mixture of H_2, CO, and Ne.

In experiments in which an unreduced Fe_2O_3/Mn_2O_3 precipitated catalyst was directly exposed to the same gas mixture at 9.2 kPa and at 525 K, no hydrocarbon formation and only a slow reduction were observed. The reduced and subsequently pre-

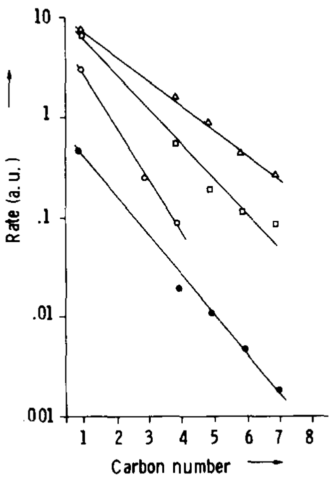

FIG. 7. Schulz–Flory plot of the hydrocarbon product distribution after Fischer–Tropsch synthesis in the batch reactor. Synthesis: $T = 523$ K; $P_{H_2} = 5.5$ kPa; $P_{CO} = 1.4$ kPa. After 1 ks of synthesis: on a reduced catalyst, ○; on an oxygen-pretreated catalyst (40 μmol O_2 for 1.7 ks), △; on an oxygen-pretreated catalyst (78 μmol $^{18}O_2$ for 12 ks), □. After 35 ks of synthesis on a reduced catalyst, ●.

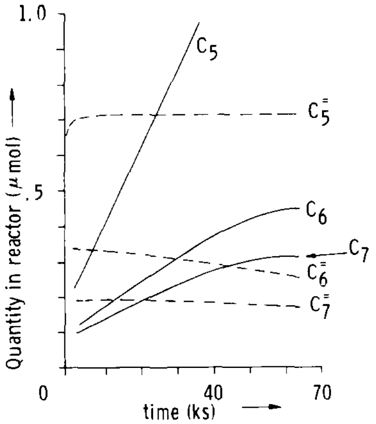

FIG. 9. C_5–C_7 olefin (C_n^{2-}) and paraffin (C_n) concentrations during Fischer–Tropsch synthesis in the batch reactor on a reduced catalyst after a pretreatment with 40 μmol O_2 for 1.7 ks. $T = 523$ K; $P_{H_2} = 5.5$ kPa; $P_{CO} = 1.4$ kPa.

oxidized catalysts however produced immediately methane, the production of which increased during the consecutive reaction period. No induction period, as observed with the untreated reduced iron catalysts, was observed. In Fig. 7 the product distribution on the preoxidized catalyst is shown after a reaction period of 1 ks. Figure 8 shows, as a basis for comparison, the formation of the C_5–C_7 products on a reduced catalyst. Figure 9 shows the same data for a preoxidized catalyst. The formation of the oxygen-containing compounds on the preoxidized catalyst is given in Fig. 10. From atomic mass balances the quantities of carbon and oxygen remaining on the catalyst are calculated and reported in Fig. 11.

DISCUSSION

If the quantity of CO adsorbed at room temperature on the catalyst used in this study, 60 μmol CO/g Fe (*1*), is indicative of one monolayer, we find from the data of Fig. 3 that in the low-pressure experiment the equivalent of about 0.05 monolayer of carbon and of oxygen is adsorbed or absorbed when the maximum rate of benzene formation is reached (15 ks). This means that for CO the sticking probability must be very low, as under the existing conditions the minimum time to form a monolayer of carbon monoxide would be less than 0.2 ms. It is remarkable that although the carbon surface coverage is small, the catalyst converts more carbon monoxide into higher hydrocarbons than, e.g., into methane, except at the very beginning, when, presumably with the aid of the hydrogen left on the catalyst after reduction, the methane production is the highest, as can be seen in Fig. 2. We are of the opinion that, although for the formation of olefins and especially of aromatics less hydrogen is needed than for the formation of paraffins, the high fraction of olefins and aromatics in the output can only be explained partly by a lack of hydrogen. Because there is no reason to assume that the hydrogen concentration on the surface increases during an experiment, we conclude that the slow but steady increase in the production of normal Fis-

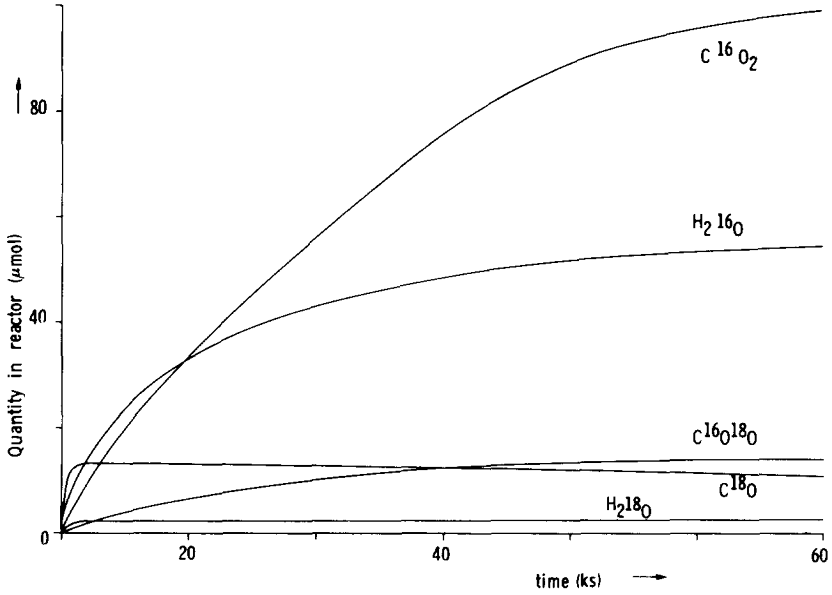

FIG. 10. Concentrations of unlabeled and ^{18}O-labeled products during Fischer–Tropsch synthesis in the batch reactor on a reduced catalyst after a pretreatment with 78 μmol $^{18}O_2$ for 12 ks. $T = 523$ K; $P_{H_2} = 5.5$ kPa; $P_{CO} = 1.4$ kPa.

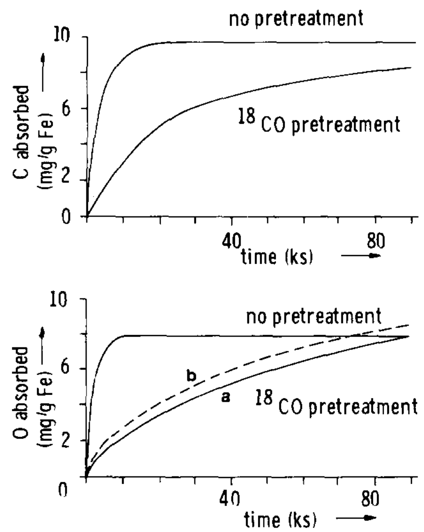

FIG. 11. Uptake of carbon and oxygen during Fischer–Tropsch synthesis in a batch reactor on a reduced catalyst with no pretreatment and on a reduced catalyst, pretreated with 78 μmol/g $^{18}O_2$. T = 523 K; P_{H_2} = 5.5 kPa; P_{CO} = 1.4 kPa. (a) Net ^{16}O uptake on pretreated catalyst; (b) ^{16}O uptake, after correction for ^{18}O desorption.

cher–Tropsch products is caused by the formation of an increasing number of sites that are active in the hydrogenation of carbonaceous surface species. The initially high rate of aromatics formation thus might be due to a lack of these hydrogenating surface sites at the beginning of the experiment. However, because the aromatics formation is not at all in agreement with the Schulz–Flory distribution we do not think that these products are formed according to the customary chain growth model, but that they are formed from six-membered carbon rings laid down on the surface. In this connection it is worth mentioning that graphitic 6-rings fit very well on a layer of close-packed iron atoms, when the carbon atoms are located in the valleys between three adjacent iron atoms: the shortest distance between the centres of two of these valleys is 0.143 nm, and the graphitic C–C distance is 0.142 nm (*7*).

At the maximum benzene formation rate there is only a small fraction (not more than 5%) of the surface covered by carbon. If this carbon were randomly distributed, only a negligible fraction would be in the form of C_6 rings. The relatively exceptionally high rate of benzene formation thus suggests that a selective adsorption process is operative in which carbon adsorption is favoured at sites adjacent to sites that are already occupied with carbon. This formation of aromatics from surface carbides is reminiscent of the original mechanistic model of Fischer and Tropsch (*8*). In the 9.2-kPa experiment much more carbon and oxygen is taken up by the catalyst as is shown in Fig. 5. The quantities shown correspond to about 13 monolayers of carbon and about 8 monolayers of oxygen, but we assume that most of the deposited material is transferred to the bulk of the catalyst. The rates of formation of hydrocarbons remained reasonably constant in this experiment as follows from the straight lines in Fig. 4. This can be ascribed to the approximately zero order of the reaction rate in carbon monoxide. We found this zero order also under atmospheric conditions (*1*). It follows from a hydrogen mass balance that the hydrogen concentration in the gas phase decreased only marginally during the experiment.

Two reasons may be offered as an explanation for the almost negligible rate of benzene formation in this experiment. One is that so much carbon is present on the surface that almost no isolated six-membered rings are present; the other is that the higher hydrogen pressure and the higher carbon deposition both enhance the formation of paraffins and olefins at the cost of the formation of aromatics. For instance, the rate of methane formation increases from 2 × 10^{-13} mol/g cat · s at a pressure of 24 Pa to 4 × 10^{-10} mol/g cat · s at 9.2 kPa. During the "induction" period of about 15 ks predominantly olefinic C_3 and C_4 hydrocarbons were observed, but the paraffin/olefin ratio increased during the consecutive activation period, as was also found with this catalyst at atmospheric pressure (*9*). At 9.2 kPa a normal Fischer–Tropsch reaction model was operative, as can be concluded from the product distribution shown in Fig. 7.

The C_2 and C_3 determinations are hindered by the spectral signals from carbon monoxide, carbon dioxide, and fragments of the higher hydrocarbons. Therefore these data are often omitted from our results.

Initially more oxygen was removed in the form of water than as carbon dioxide (Fig. 6). After about 15 ks the concentration of water in the reactor started to fall, while the carbon dioxide concentration continued to increase. From the oxygen mass balance we conclude that after 10 ks no further oxygen was taken up by the catalyst, so that the observed decrease of the water content is coupled to the increase of the carbon dioxide concentration: due to the long reaction time in the batch reactor the equilibrium of the water-gas shift reaction, which under our conditions lies on the CO_2 side (*10*), is approached.

From Fig. 7 we see that the activity levels of the two preoxidized catalysts are higher than that of the untreated one, but that the influence of the smaller quantity of oxygen is more pronounced than that of the higher quantity. This means that two opposing effects are operating, an activating one at low oxygen content and a deactivating one at a higher oxygen content. The inactivity of an unreduced iron catalyst can be mentioned in this connection. Another interesting observation follows from the comparison of Figs. 8 and 9. Figure 8 shows the normal behaviour of an untreated reduced iron catalyst, viz., slow activation and an increase in both olefinic and paraffinic products. The rate of increase is greater for the paraffins than for the olefins. In Fig. 9 we see that olefins are only formed at the very beginning of the experiment, and then at a rather high rate. This means that in the sequence

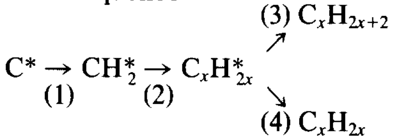

$$C^* \xrightarrow[(1)]{} CH_2^* \xrightarrow[(2)]{} C_xH_{2x}^* \begin{array}{l} \nearrow (3)\ C_xH_{2x+2} \\ \searrow (4)\ C_xH_{2x} \end{array} \qquad (1)$$

all steps except (3) proceed in the initial stage of the synthesis at a high rate. However, as follows from Fig. 7, the methane rate is not depressed at all. This suggests that the two steps

$$CH_2^* + 2H^* \rightarrow CH_4 \qquad (2)$$

and

$$C_xH_{2x}^* + 2H^* \rightarrow C_xH_{2x+2} \qquad (3)$$

are different in nature: the rate of Eq. (2) has a normal value on a lightly oxidized catalyst whereas the rate of Eq. (3) is very much inhibited. This means that the hydrogenation ensembles active for the elementary steps (2) and (3) must be different. This initial inhibition of the higher paraffin formation results in a decrease of the overall termination rate constant, and thus in a smaller Schulz–Flory constant α.

Figure 10 shows into what types of exchange the preadsorbed ^{18}O can enter: formation of $C^{18}O$, $C^{18}O^{16}O$, and $H_2{}^{18}O$ and even a very small quantity of $C^{18}O^{18}O$. The slight decrease in the concentrations of hexene and heptene, shown in Fig. 9, indicates the possibility of readsorption of these olefins followed by hydrogenation.

The formation of $C^{18}O$ must occur according to an equilibrium reaction as

$$C^* + {}^{18}O^* \leftrightarrows C^{18}O + 2^*. \qquad (4)$$

The rate of formation of $C^{18}O$ in the initial period is high (6.5 nmol/g cat · s) as compared to the Fischer–Tropsch reaction rate on such a catalyst. From Fig. 4 we calculate a total Fischer–Tropsch rate under the same conditions of about 1 nmol CO converted/g cat · s. This shows that under the conditions applied in this study the CO dissociation rate is much higher than the Fischer–Tropsch reaction rate. It shows at the same time that the interaction of gaseous carbon monoxide with surface oxygen can be more complex than assumed by Van Ho and Harriott (*11*) in their study on nickel. For as follows from Fig. 10, the $C^{16}O^{18}O$ formation rate is much lower than the $C^{18}O$ formation rate. Thus on iron the rate of CO_2

formation is not at all indicative of the CO dissociation rate, whereas on nickel according to Van Ho and Harriott the CO_2 formation rate is a measure of the CO dissociation rate.

As far as the carbon dioxide and water formation rates are concerned, we see that the rates of the unlabeled products are much higher than those of the products containing an ^{18}O atom, while for labeled and unlabeled products the carbon dioxide formation is higher than the water formation. From the former observation we conclude that much less ^{18}O than ^{16}O is available for exchange.

From a comparison of the quantities of carbon and oxygen adsorbed during the Fischer–Tropsch synthesis on a reduced and on the ^{18}O-pretreated catalyst (Fig. 11) we see that the predeposition of oxygen hinders the subsequent deposition of carbon and oxygen from synthesis gas. From the exchange experiments shown in Fig. 10 we estimate that 54 μmol ^{18}O/g Fe (corresponding to about one monolayer) is available for exchange. From hydrogen stripping experiments at 523 K we have found that at that temperature only part of the total oxygen deposited on and in a catalyst can be recovered as water. Since the exchange reaction was fast, the exchanged oxygen must be present in the outer layer of the catalyst.

CONCLUSIONS

From the observations described in the previous section the following conclusions can be drawn:

(i) Carbon monoxide adsorbs dissociatively on iron, and this dissociation is a fast reaction. This follows from the experiment with labeled oxygen, where the carbon monoxide dissociation rate appears to be much faster than the carbon dioxide formation rate or the total rate of Fischer–Tropsch conversion on a normal catalyst (Figs. 10 and 4).

(ii) The hydrogenation mechanisms for methane formation and for the formation of the higher paraffins are not the same. This follows mainly from a comparison of the product distributions on a reduced catalyst and on a preoxidized catalyst.

(iii) There are indications that active carbon atoms adsorbed on the surface of the catalyst facilitate the deposition of other active carbon atoms on neighbouring sites. This follows from the relatively high rate of aromatic formation at 24 Pa.

A comparable conclusion can be drawn from the experiments of Araki and Ponec (*12*) on nickel. Their experiments show that the formation of $^{12}CH_4$ from ^{12}CO and H_2 is enhanced when first some ^{13}C is deposited on the catalyst.

(iv) Oxygen adsorbed on the catalyst

—inhibits the deposition of carbon (Fig. 11);

—activates the Fischer–Tropsch reaction on an iron catalyst (Figs. 7 and 9);

—increases the probability of chain growth (α) (Fig. 7).

Dwyer and Somorjai (*13*) also observe a higher initial reaction rate with preoxidized iron catalysts, and also a small shift towards higher-molecular-weight products. Somorjai and co-workers (*3, 14*) observe the same phenomena on polycrystalline Rh foils. The increased reaction rate after an oxygen pretreatment is also observed by various authors on other metals such as nickel and cobalt (*15*) and ruthenium (*16, 17*).

It is known that extensive oxygen penetration in the lattice of iron can already occur at 85 K (*18, 19*). Boudart (*20*) has suggested that oxygen which penetrates into the outer layers of the catalyst causes, as follows from photoelectric measurements, a lowering of the work function. This can result in an increased adsorption of hydrogen. This latter phenomenon is also observed on iron catalysts by Burshtein and Surova (*21*). More recent results of Chesters and Rivière (*22*) have shown that a lowering of the work function only occurs after a room-temperature exposure of more than 20 Langmuirs (0.0025 Pa s). In our experiments the exposure has always been many orders of magnitude higher.

Furthermore it has been observed by various authors (*23–25*) that the presence of negative ions (halides, sulfide, oxide) reduces the carbon–metal bond strength and in this way hampers the formation of carbon deposits (see Fig. 11). This allows for more stable operation of such catalysts at higher temperatures.

REFERENCES

1. van Dijk, W., Thesis, Eindhoven University of Technology, 1981.

2. Tillmetz, K. D., Thesis, University of Technology, Berlin, 1976.

3. Sexton, C. A., and Somorjai, G. A., *J. Catal.* **46,** 167 (1977).

4. van Lith, W., Sommen, A. P. B., and van Dijk, W., to be published.

5. Efroymson, M. A., and Jenrich, R. I., *in* "Statistical Methods for Digital Computers" (A. Ralston and H. S. Wilf, Eds.), Vol. 3. Wiley, New York, 1977.

6. Henriquez, L., M.Sc. report, Eindhoven University of Technology, 1980.

7. West, R. C. (Ed.), "Handbook of Chemistry and Physics," 46th ed., pp. F 118, 119, The Chemical Rubber Co., Cleveland, Ohio, 1965.

8. Fischer, F., and Tropsch, H., *Brennst. Chem.* **7,** 97 (1926).

9. van Dijk, W., van der Baan, H. S., Niemantsverdriet, J. W., and van der Kraan, A. M., *Appl. Catal.*, in press.

10. Anderson, R. B., *in* "Catalysis" (P. H. Emmett, Ed.), Vol. IV, p. 1. Reinhold, Baltimore, 1956.

11. Van Ho, S., and Harriott, P., *J. Catal.* **64,** 272 (1980).

12. Araki, M., and Ponec, V., *J. Catal.* **44,** 439 (1976).

13. Dwyer, D. J., and Somorjai, G. A., *J. Catal.* **52,** 291 (1978).

14. Castner, R. G., Blachader, B. L., and Somorjai, G. A., *J. Catal.* **66,** 257 (1980).

15. Palmer, R. L., and Vroom, D. A., *J. Catal.* **50,** 244 (1977).

16. Dalla Betta, R. A., Shelef, M., and Piken, A. G., *J. Catal.* **35,** 54 (1974).

17. King, D. L., *J. Catal.* **51,** 386 (1978).

18. Quinn, C. M., and Roberts, M. W., *Trans. Faraday Soc.* **58,** 569 (1962).

19. Roberts, M. W., *Trans. Faraday Soc.* **57,** 99 (1961).

20. Boudart, M., *J. Amer. Chem. Soc.* **74,** 3556 (1952).

21. Burshtein, R. R., and Surova, M. D., *Dokl. Akad. Nauk. SSSR* **61,** 75 (1948).

22. Chesters, M. A., and Rivière, J. C., *in* "Proceedings, 7th Intern. Vac. Congr. & 3rd Intern. Conf. Solid Surface, Vienna, 1977," p. 873.

23. Kieffer, E. Ph., Thesis, Eindhoven University of Technology, 1981.

24. Davis, H. G., and Wilson, T. P., U.S. Patents 2717259, 2717250 (1955).

25. Hammer, H., and Bittner, D., *Erdoel Kohle* **31**(8), 369 (1978).